Geophysical Research Letters

RESEARCH LETTER
10.1029/2025GL117386

Radiative and Precipitation Processes Make it Easier to Match the Temperature Record and Harder to Constrain Future Warming

Ci Song[1], Geethma Werapitiya[1], Daniel T. McCoy[1], Duncan Watson-Parris[2], Andrew Gettelman[3], and Trude Eidhammer[4]

[1]Department of Atmospheric Science, University of Wyoming, Laramie, WY, USA, [2]Scripps Institution of Oceanography and Halicioğlu Data Science Institute, University of California San Diego, La Jolla, CA, USA, [3]Pacific Northwest National Laboratory, Richland, WA, USA, [4]NSF National Center for Atmospheric Research, Boulder, CO, USA

Abstract By examining the historical temperature record during the industrial era, we can infer the climate's sensitivity to radiative perturbations, given knowledge of historical forcings. Energy conservation enforces a negative correlation between the climate feedback and historical forcing for a given change in global-mean temperature. Here, we examine the negative correlation between the radiative forcing due to aerosol-cloud interactions and the shortwave cloud feedback to warming that appears in a perturbed parameter ensemble (PPE). The PPE is not tuned to match the historical record, yet a negative correlation emerges over the extratropics due to the combined effects of liquid cloud precipitation efficiency and radiative saturation in the shortwave. Using an energy balance model, we argue that these processes combine to push Earth System Models to yield a temperature record in keeping with observations, but also limit our ability to constrain future warming posterior with the temperature record.

Plain Language Summary Clouds play an important role in Earth's energy budget by reflecting solar radiation back to space and by absorbing and re-emitting thermal radiation. As the planet warms, cloud properties may change, which can either amplify or dampen global warming—a process known as cloud feedback. In addition to changes caused by warming, aerosols interact with clouds in complex ways, further modifying cloud properties. This is referred to as aerosol–cloud interactions. Understanding how clouds respond to both warming and changing aerosol emissions, and how these responses affect radiation is critical for constraining future climate projections. In this study, we examine the changes in cloud properties and radiation in response to warming and aerosol perturbations using a climate model run many times with modified parameters. The results show that the radiative response to both warming-induced and aerosol-induced cloud changes is primarily governed by how efficiently clouds convert their water content into precipitation. In this context, we illustrate how the interplay of cloud, precipitation, and radiative processes affect the ability of models to match the historical temperature record and in turn, how the historical temperature record can be used to provide constraint on future warming.

Key Points:

- Precipitation efficiency drives both cloud radiative saturation and cloud macrophysical responses to aerosol and warming
- Radiative saturation driven by precipitation efficiency leads to a negative correlation between forcing and feedback
- This anticorrelation makes it easier for models to match the historical record but harder to constrain future temperature projections

Supporting Information:

Supporting Information may be found in the online version of this article.

Correspondence to:

C. Song,
csong@uwyo.edu

Citation:

Song, C., Werapitiya, G., McCoy, D. T., Watson-Parris, D., Gettelman, A., & Eidhammer, T. (2025). Radiative and precipitation processes make it easier to match the temperature record and harder to constrain future warming. *Geophysical Research Letters*, *52*, e2025GL117386. https://doi.org/10.1029/2025GL117386

Received 5 JUN 2025
Accepted 27 NOV 2025

Author Contributions:

Conceptualization: Ci Song, Geethma Werapitiya, Daniel T. McCoy, Andrew Gettelman
Formal analysis: Ci Song, Geethma Werapitiya, Daniel T. McCoy
Funding acquisition: Daniel T. McCoy
Investigation: Ci Song, Geethma Werapitiya, Daniel T. McCoy, Duncan Watson-Parris, Andrew Gettelman

1. Introduction

Clouds play an important role in regulating Earth's energy budget. The radiative response at the top of the atmosphere (TOA) due to the presence of clouds is referred to as cloud radiative effect (CRE: W/m^2). The net CRE on Earth's climate depends on cloud type, altitude, and coverage (Boucher et al., 2013). As the planet warms with increasing greenhouse gases (GHGs) emissions, the change in cloud properties in response to warming may lead to the change in TOA radiative flux (ΔCRE) and consequently an amplified or dampened global warming, known as cloud feedback (λ_{cld}: $W/m^2/K$) (Zelinka et al., 2020). Cloud feedback is the primary source of uncertainty in the total radiative feedback response to increasing GHGs, which is composed of cloud feedback λ_{cld} and non-cloud feedback λ_{noncld} (Ceppi et al., 2017; Eyring et al., 2016; Taylor et al., 2012; Zelinka et al., 2020), given by

$$\lambda = \lambda_{cld} + \lambda_{noncld} \quad (1)$$

where the non-cloud feedbacks λ_{noncld} arise from changes in water vapor, surface albedo and atmospheric temperature (B. J. Soden & Held, 2006). They are less uncertain relative to cloud feedback.

Methodology: Ci Song, Geethma Werapitiya, Daniel T. McCoy, Duncan Watson-Parris, Andrew Gettelman, Trude Eidhammer
Project administration: Daniel T. McCoy
Resources: Geethma Werapitiya, Daniel T. McCoy, Duncan Watson-Parris
Software: Duncan Watson-Parris, Andrew Gettelman, Trude Eidhammer
Supervision: Daniel T. McCoy
Validation: Ci Song, Geethma Werapitiya, Daniel T. McCoy, Trude Eidhammer
Visualization: Ci Song, Geethma Werapitiya, Daniel T. McCoy
Writing – original draft: Ci Song
Writing – review & editing: Ci Song, Geethma Werapitiya, Daniel T. McCoy, Duncan Watson-Parris, Andrew Gettelman, Trude Eidhammer

In addition to cloud response to warming, anthropogenic aerosols provide an additional mechanism for inducing cloud changes. Aerosols can act as cloud condensation nuclei during cloud formation, altering the Earth's energy budget through changes in cloud properties (ACI: aerosol-cloud interactions). First, aerosols may change cloud reflectivity through changes in cloud microphysical properties such as cloud droplet number concentration (Nd) and cloud droplet size (Twomey, 1977). Second, cloud macrophysics (cloud extent and the amount of cloud condensate) may be altered due to change in Nd and cloud droplet size (Ackerman et al., 2004; Albrecht, 1989). The change in TOA radiative flux due to the combined effects from changes in cloud microphysics and macrophysics is the effective radiative forcing due to ACI (ERF_{aci}: W/m^2) (Bellouin et al., 2020). ERF_{aci} is the leading source of uncertainty in the total radiative forcing from aerosols ERF_{aer}, given in

$$ERF_{aer} = ERF_{ari} + ERF_{aci} \tag{2}$$

The direct radiative forcing from aerosol-radiation interactions (ERF_{ari}) is less uncertain and contributes less to ERF_{aer} than ERF_{aci} (Bellouin et al., 2020; C. J. Smith et al., 2020). ERF_{aci} and cloud feedback can each be further decomposed into shortwave and longwave components. In this study, we focus our analysis on the shortwave component of both ERF_{aci} and cloud feedback λ_{cld}, which is the dominant source of intermodel spread (Bellouin et al., 2020; Sherwood et al., 2020; Zelinka et al., 2020).

Previous studies have examined the relationship between ERF_{aci} and λ_{cld}. A negative correlation between ERF_{aci} and λ_{cld} has been found in fully-coupled Earth System Models (ESMs) (Andrews et al., 2012; Kiehl, 2007; Wang et al., 2021; Webb et al., 2013). Wang et al. (2021) suggest that the negative correlation between λ_{cld} and ERF_{aci} across ESMs may be a result of tuning cloud-related parameters. This tuning can occur either explicitly, by adjusting parameters directly, or implicitly, through modifications to model physics during development when the climate sensitivity appears unrealistic. As a result, ESMs may be tuned to have more positive λ_{cld} and more negative ERF_{aci}, or vice-versa as a result of energy conservation (Mauritsen et al., 2012). The concept of energy conservation means that the relationship between the global-mean near-surface air temperature response ΔT, radiative forcing ΔF, and climate feedback parameter λ can be related using

$$\Delta N = \Delta F + \lambda \Delta T \tag{3}$$

where ΔN is the net TOA radiative flux anomaly. Considering TOA radiative flux perturbations only resulting from cloud changes, the total cloud radiative response ΔCRE_{tot} can be decomposed into the radiative response from changes in clouds driven by surface warming (i.e., cloud feedback) and ACI (Wang et al., 2021; B. Soden & Chung, 2017), given by

$$\Delta CRE_{tot} = ERF_{aci} + \Delta CRE_{warming} \tag{4}$$

We note that ΔCRE_{tot} here includes cloud masking effect: the presence of clouds tends to obscure part of the radiative effects of non-cloud feedbacks (B. J. Soden et al., 2004). We do not attempt to separate the masking effect from the true cloud feedback in this work. Assuming the cloud radiative response to warming is proportional to global-mean surface warming (Gregory et al., 2004), the cloud radiative response to warming can be estimated by cloud feedback parameter multiplied by surface temperature perturbation

$$\Delta CRE_{tot} = ERF_{aci} + \lambda_{cld} \Delta T \tag{5}$$

As a result, ERF_{aci} and λ_{cld} tend to be anti-correlated when models are forced to match with historical records (e.g., ΔCRE_{tot}, ΔT) by turning parameters in fully-coupled ESMs. This equation is intended as an illustration. In practice, climate models are more commonly tuned to match the TOA radiation balance and surface temperature (i.e., ΔT), rather than changes in CRE. ΔCRE remains too uncertain observationally to serve as direct tuning targets. However, tuning cloud-related parameters to match the historical record may implicitly lead to agreement with observed changes in CRE (ΔCRE).

Instead of looking at fully-coupled ESMs, we examine ERF_{aci} and cloud feedback λ_{cld} using a Perturbed Parameter Ensemble (PPE) from the Community Atmosphere Model version 6 (CAM6). A negative correlation between global mean shortwave cloud feedback λ_{cld} and global mean ERF_{aci} emerges across the CAM6 PPE, for

which parameters are not tuned with the intention of matching historical record across simulations (Figure S1a in Supporting Information S1). As in Gettelman et al. (2024), there is substantial spread among ensemble members, but there is a statistically robust relationship that emerges between these terms. The result indicates that the negative correlation between λ_{cld} and ERF_{aci} is insensitive to constraining TOA flux to observations.

Gettelman et al. (2024) traced the negative correlation to cloud and precipitation processes. Here we examine this behavior in the context of recent work highlighting how precipitation and cloud processes couple with radiation (Song et al., 2024). Unlike Song et al. (2024) that primary focus on the radiative buffering on aerosol forcing, this work provides a physically based explanation of how radiative buffering simultaneously influences both aerosol forcing and cloud feedback and examine how this dual role contributes to their negative correlation.

Finally, in the context of a zero-dimensional energy balance model (Forster, 2016), we illustrate how the interplay of cloud, precipitation, and radiative processes affects the ability of ESMs to match the historical temperature record and in turn of the historical temperature record to provide constraint on future warming.

2. Data and Methods

2.1. CAM6 Perturbed Parameter Ensemble

CAM6 is the atmosphere component of the Community Earth System Model 2 (CESM2) (Danabasoglu et al., 2020). The CAM6 allows a two-moment microphysics scheme for stratiform cloud microphysics for which cloud hydrometers (e.g., liquid droplets, ice crystals, rain and snow) are calculated using prognostic equations (Gettelman et al., 2015). It permits more realistic representations on the number concentration and mass mixing ratio of hydrometers than one-moment microphysics scheme, thus a more robust interaction between aerosols, clouds, and radiation.

A PPE is created with CAM6. A PPE is an ensemble of simulations with unique parameter combinations within a defined parameter range based on expert-elicitation. In this study, CAM6 PPE is perturbed with 45 parameters related to aerosols, their activation, cloud microphsics, turbulence, and convection. It consists of 262 simulations with combinations of 45 parameters sampled from latin hypercube, enabling efficient coverage of parameter space (Eidhammer et al., 2024). A full list of perturbed parameters is given in Table S1 in Supporting Information S1.

We evaluate cloud radiative response from changes in clouds driven by surface warming (i.e., cloud feedback) using paired Present-day (PD) and SST4k (i.e., SST uniformly increased by 4K) simulations. PD and SST4K simulations are completed using the same model configuration and parameter sets except setting the SST uniformly increased by 4K in SST4K simulations (Cess et al., 1989). The detailed model configuration can be found in Eidhammer et al. (2024).

To evaluate cloud radiative response due to anthropogenic aerosols, we use paired preindustrial (PI) and PD simulations integrated for 2 years from 2019 to 2020. We note that 2020 was a weak El Niño, but we believe it has minimal impact on our results, as we analyze 2-year and extratropical-averaged aerosol forcing and cloud feedback, which helps reduce the impact of short-term and internal variability. Furthermore, the anticorrelation identified in the PPE is also evident in fully coupled model ensembles with 50-year simulation (Wang et al., 2021), suggesting that it is a robust feature. In these simulations, the atmosphere is nudged to horizontal winds and temperature from the NASA Modern-Era Retrospective analysis for Research and Applications, Version 2 (MERRA2) (Molod et al., 2015) as detailed in Song et al. (2024). SSTs are also prescribed from the MERRA-2 reanalysis. This setup suppresses the surface temperature feedback and limits the potential for regional feedbacks initiated by aerosol perturbations. PI simulations are completed using the same model configuration and parameter sets as PD except setting the aerosol emissions to 1850 levels. Nudging configuration is needed for the calculations of aerosol forcing as it reduces the variability in aerosol forcing induced by meteorological variabilities. In our setup, 2-year integration is able to produce a stable aerosol forcing without additional years of simulations, while extending to longer simulations would be computationally expensive (Song et al., 2024). One caveat to our analysis is that all simulations are run in atmosphere-land mode as opposed to fully-coupled. Coupling PPE members is usually not possible (Sexton et al., 2021) and if possible, computationally expensive. Early studies pointed to disconnects between uniform warming (Cess-type) cloud feedbacks and the feedback calculated from fully-coupled models (Ringer et al., 2006; Senior & Mitchell, 1993). However, studies of modern ESMs suggest that the correspondence

between the feedback simulated by fully-coupled and Cess-type simulations is substantially stronger than previously reported (Qin et al., 2022).

2.2. Analysis Approach

For each paired simulations (i.e., PD and SST4K, PD and PI), we evaluate their cloud macrophysical property response and cloud radiative response to surface warming and aerosols. The variables analyzed in this study are detailed in Text S1 and Table S2 in Supporting Information S1.

The goal of this study is to characterize the interaction between cloud radiative response to surface warming and aerosols using precipitation and cloud radiative processes. Precipitation efficiency describes how effectively a certain amount of water condensate in a cloud can be converted into precipitation (Li et al., 2022), given in

$$PE = \frac{P_s}{CWP} \tag{6}$$

where CWP is the condensed water path, which represents the column-integrated cloud liquid and ice content. P_s is the surface precipitation including both liquid and ice precipitation. A full list of CAM6 PPE variables analyzed in this study is given in Table S2 in Supporting Information S1.

We restrict our study domain in extratropics in both hemispheres. The extratropics is a region of moisture convergence in the present-day climate (McCoy et al., 2022), which is also evident in the CAM6 PPE simulations (Figure S2 in Supporting Information S1). We choose this region because the Northern extratropics dominate ERF_{aci} (Song et al., 2024; Wall et al., 2022) and because of the large inter-model spread in extratropical shortwave feedback in the Southern Hemisphere (Zelinka et al., 2020). The tropics are also a region of strong moisture convergence but are excluded from our reanalysis because ESMs don't typically include aerosol-cloud interactions in deep convection, which makes it hard to interpret results. We examine the CRE in the extratropics in both hemispheres in the CAM6 PPE in the latitude range of 50° to 80° (Figure S2 in Supporting Information S1), although extending the study region to global does not significantly change the results.

2.3. Energy Balance Model

We illustrate how the correlations between ERF_{aci} and cloud feedback, driven by the interplay of cloud, precipitation, and radiative processes, affect the ability of ESMs to match the historical temperature record. We also show the role of correlations in constraining future warming with historical temperature record.

Finite amplitude Impulse Response version 2 (FaIRv2.0) is a highly parameterized, zeroth-dimension model that simulates globally averaged variables (Leach et al., 2021). We use the FaIRv2.0 energy balance model to simulate temperature predictions under different combinations of ERF_{aci} and cloud feedback. Following Watson-Parris (2025); Cummins et al. (2020), the configuration of FaIR model is tuned to match the deep-ocean heat uptake simulated from fully-coupled CESM2 model. The parameters used in this study are in Table S3 in Supporting Information S1, consistent with the setting in Watson-Parris (2025).

We generate 1,000 paired samples of ERF_{aci} and cloud feedback from a bivariate normal distribution. This is intended to represent a prior on what a plausible climate model might look like in terms of its representation of ERF_{aci} and cloud feedback processes. The distributions capture the uncertainty ranges of ERF_{aci} and cloud feedback reported in 6th Assesment Report (AR6). To explore how correlations between ERF_{aci} and cloud feedback impact ESMs to predicting future temperature, we generate 3 sets of 1,000 paired samples of ERF_{aci} and cloud feedback with imposed correlation coefficients of 0.6, −0.6, and 0 (Figure S3 in Supporting Information S1).

To simulate historical temperature projections under the assumptions of different correlations between ERF_{aci} and cloud feedback, we derive ERF_{aci} as a function of emissions for each scenario of correlation ($ERF_{aci}(E)$) following the scaling method from Watson-Parris (2025), given by

$$ERF_{aci}(E) = ERF_{aci}(E0)\left(\frac{ERF_{aci}}{ERF_{aci}(0)}\right) \tag{7}$$

Where $ERF_{aci}(0) = -0.84$ W/m^2 is the central estimate from AR6 (C. Smith et al., 2021). ERF_{aci} is from the jointly sampled 1,000 ERF_{aci} in a normal distribution. $ERF_{aci}(E0)$ is the time-series of ERF_{aci} from AR6 best estimate (Watson-Parris, 2025; C. Smith et al., 2021). The total imposed forcing in the FaIR model is the sum of the forcing from ACI contributions and the non-ACI components

$$ERF_{tot} = ERF_{aci}(E) + ERF_{nonaci}(E) \tag{8}$$

where $ERF_{nonaci}(E)$ is calculated from AR6 best estimate ERF (C. Smith et al., 2021). The total climate feedback λ_{tot} is estimated as the default total climate feedback $\lambda_{tot,0}$, add the difference between the jointly sampled cloud feedback λ_{cld} and the default cloud feedback $\lambda_{cld,0}$ following Watson-Parris (2025).

$$\lambda_{tot} = \lambda_{tot,0} + \lambda_{cld} - \lambda_{cld,0} \tag{9}$$

where the default total climate feedback $\lambda_{tot,0}$ is set to 0.65 in our configurative following Watson-Parris (2025), and the default cloud feedback parameter is set to 0.5 (Gettelman et al., 2019; Watson-Parris, 2025). We note that, in the FaIR model, a positive value of total climate feedback indicates stabilization, in contrast to the conventional definition where negative values imply stability. For each combination of ERF_{aci} and cloud feedback, we use FaIR model to simulate the historical and future temperature predictions. Within this set up, the simulated temperature trajectory from FaIR model is generally consistent with observational record and AR6 model estimate shown in Watson-Parris (2025).

2.4. Observational Constraints

Global mean surface temperature was 1.09°C [0.95 to 1.20°C] higher in 2011–2020 compared to 1850–1900 according to IPCC (2023). We reject samples that fail to reproduce historical global temperature change during this period.

3. Results

The ERF_{aci} calculated in this study (i.e., nudged CAM6 PPE) shows good agreement over the extratropics with the ERF_{aci} values calculated from the free-running CAM6 PPE in Gettelman et al. (2024) (Figure S4 in Supporting Information S1). Disagreement in ERF_{aci} between the two model configurations appears in tropical regions. Following Song et al. (2024), we exclude 45 PPE members from our analysis as these members results in runaway ice cloud fractions exceeding 50% over the tropics, inconsistent with satellite observations.

3.1. Cloud Responses to SST4K and Aerosols

Cloud macrophysical property changes in response to warming and anthropogenic aerosols, resulting in changes in CRE. Within extratropics, we see that the cloud radiative response to warming ($\Delta CRE_{warming}$: W/m^2) is well correlated with the macrophysical cloud response to warming SST ($\Delta LWP_{warming}$: W/m^2) with a r-value of −0.78 (Figure 1a). An increase in LWP with warming corresponds to a stronger negative feedback and vice-versa. However, the correlation between $\Delta CRE_{warming}$ and $\Delta LWP_{warming}$ degrades quickly in the negative cloud feedback (or positive $\Delta LWP_{warming}$) regime with a r-value of −0.33 (Figure 1a).

Similarly, we see a negative correlation between cloud radiative response to anthropogenic aerosol (ERF_{aci}: W/m^2) and macrophysical cloud response to aerosol ($\Delta LWP_{aerosol}$) with a r-value of −0.3. The correlation coefficient between ERF_{aci} and $\Delta LWP_{aerosol}$ is similar with the value of correlation coefficient between $\Delta CRE_{warming}$ and $\Delta LWP_{warming}$ when a positive of LWP response is simulated (Figures 1a and 1b).

As the LWP response correlates negatively with cloud radiative response in both warming- and aerosol-driven cloud changes (Figures 1a and 1b), we suspect that the relationship between $\Delta LWP_{aerosol}$ and $\Delta LWP_{warming}$ provides insight into the negative correlation between cloud feedback and ERF_{aci}. However, the correlation between $\Delta LWP_{aerosol}$ and $\Delta LWP_{warming}$ is not negative and is even slightly positive (Figure S1b in Supporting Information S1). This apparent disagreement between the LWP response correlation and the radiative response correlation suggests that additional physical processes influence the relationship between $\Delta CRE_{warming}$ and ERF_{aci}.

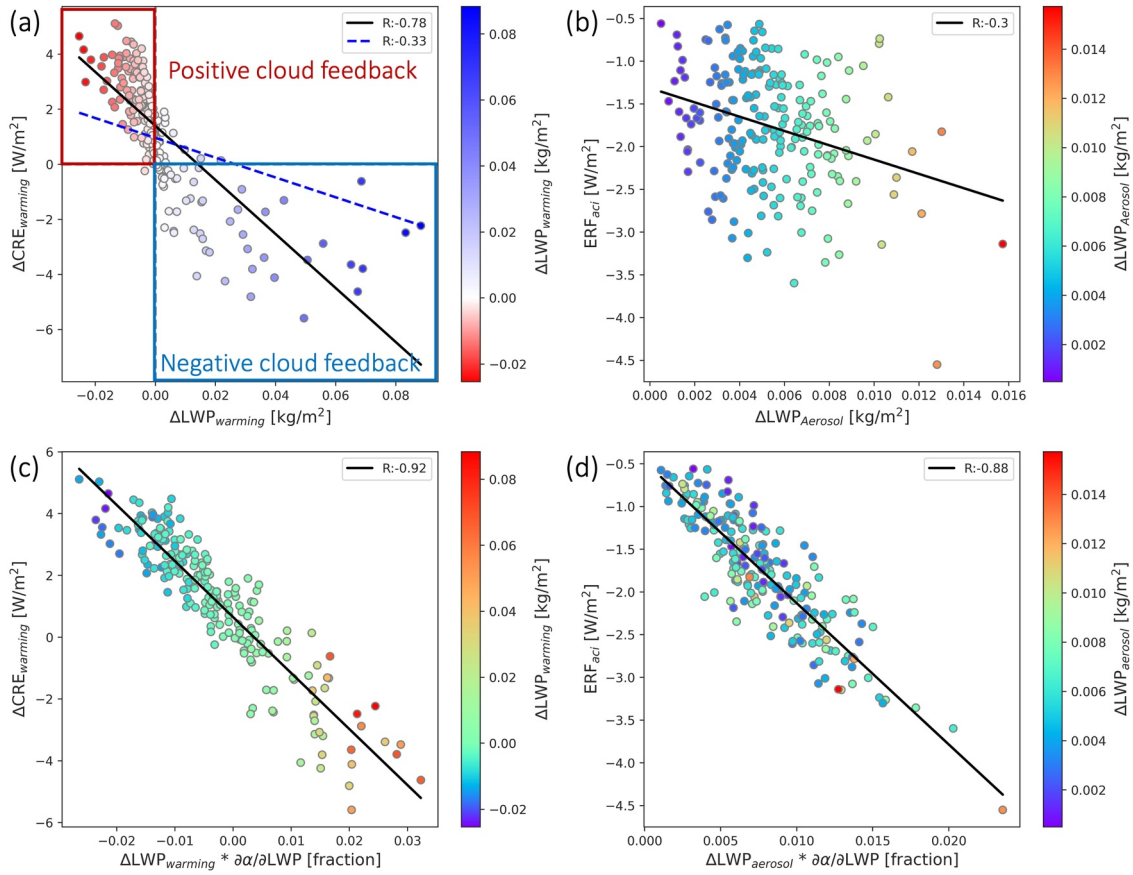

Figure 1. The cloud radiative response as a function of liquid water path (LWP) response to (a) warming and (b) aerosols and colored by LWP response across the CAM6 PPE members. (c) The cloud radiative response as a function of LWP response to warming scaled by albedo susceptibility to LWP across the CAM6 PPE members. (d) Similar to (c) but showing the cloud radiative response as a function of liquid water path response to aerosols scaled by albedo susceptibility to LWP. In (a), two regression lines are shown: the solid black line represents the linear regression across all points, while the blue dashed line represents the regression based only on points with negative cloud feedback. Both LWP and cloud radiative responses are calculated as extratropically averaged quantities over both hemispheres. LWP is grid-box averaged.

As discussed in McCoy et al. (2022) and Song et al. (2024), the scaling of cloud macrophysical processes by the sensitivity of top of atmosphere radiation to LWP is critical to understanding the $\Delta CRE_{warming}$ and ERF_{aci}, respectively. However, neither study examines the radiative buffering of both forcing and feedback together, nor the correlation between them. Building on these studies, we demonstrate that when the LWP response to anthropogenic aerosol and warming is scaled by $\partial\alpha/\partial LWP$ as defined in Song et al. (2024), strong negative correlations between the cloud radiative response and the LWP response emerge on both warming- and aerosol-driven cloud changes (Figures 1c and 1d). This suggests that the negative correlation between cloud feedback and ERF_{aci} is driven both by variation in the albedo susceptibility term $\partial\alpha/\partial LWP$, and by the response of macrophysical cloud properties to warming and aerosol perturbation. The variation in $\partial\alpha/\partial LWP$ is due to the nonlinear relationship between LWP and albedo, which has been demonstrated theoretically in Stephens (1978).

3.2. Role of Precipitation Efficiency

As suggested in Gettelman et al. (2024), precipitation processes must play a role in setting the behavior of the albedo susceptibility term and the emergent correlation between cloud feedback and ERF_{aci}. The link between precipitation efficiency (PE) and macrophysical cloud property (e.g., LWP) is shown in a strong inverse relationship across the CAM6 PPE ensembles (Figure S5 in Supporting Information S1). This relationship is reasonable to expect, as the large-scale circulation enforces a precipitation demand on the atmosphere. As precipitation efficiency decreases, the amount of cloud required to meet this demand must rise. However, as LWP rises with decreasing precipitation efficiency, the albedo susceptibility falls (Figures 2a and 2b: red dots). This is

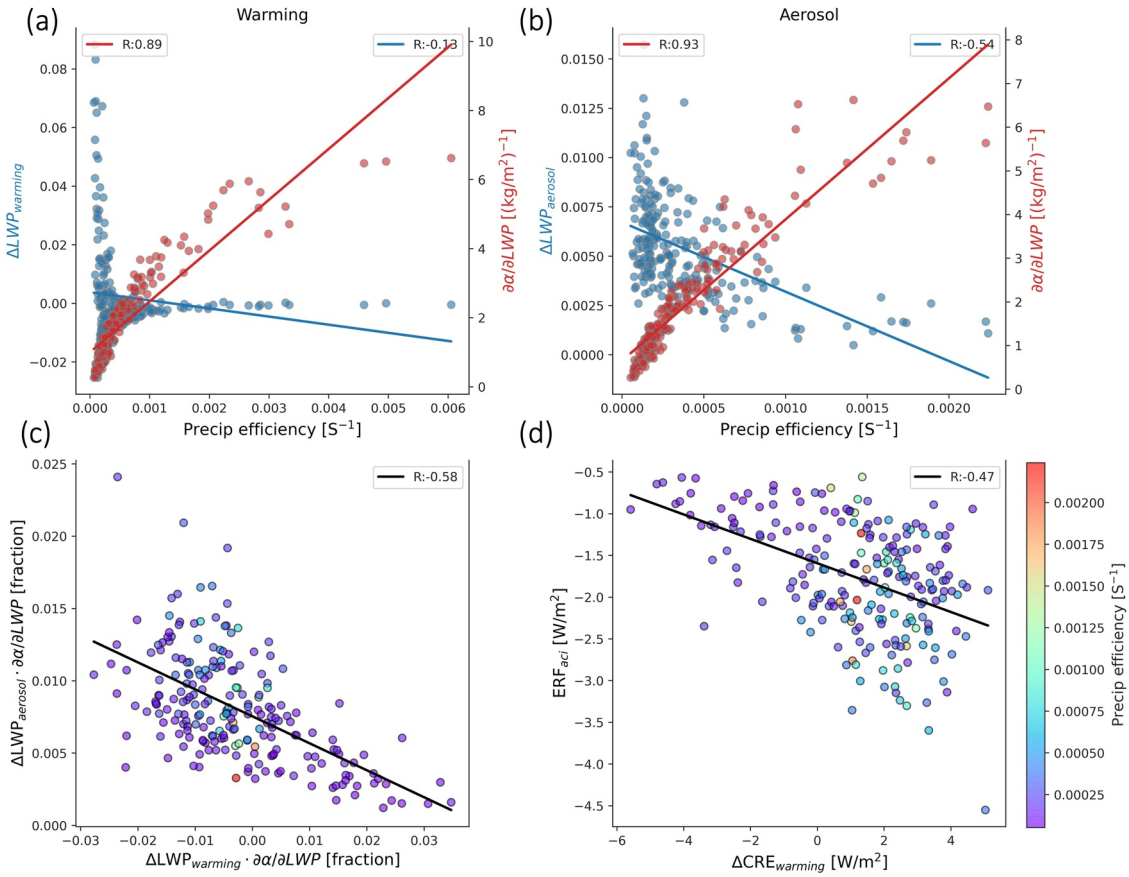

Figure 2. LWP response (ΔLWP) to (a) warming $\Delta LWP_{warming}$ and (b) aerosols $\Delta LWP_{aerosol}$ anticorrelate with albedo susceptibility ($\partial\alpha/\partial LWP$) across CAM6 PPE members as a function of precipitation efficiency. (c) The linear regression slope on $\Delta LWP_{warming}$ and $\Delta LWP_{aerosol}$ scaled by $\partial\alpha/\partial LWP$ reproduces the negative correlation between ERF_{aci} and $\Delta CRE_{warming}$ shown in (d). Precipitation efficiency, LWP and cloud radiative responses are calculated as extratropically averaged quantities over both hemispheres.

because radiative saturation has been reached and changes in LWP play a relatively unimportant role in albedo (McCoy et al., 2022; Song et al., 2024; Tan et al., 2024). The range of this behavior across the PPE is large, but not out of step with the range across recent ESMs (e.g., CMIP6: Coupled Model Intercomparison Project Phase 6) due to large inter-model spread in mean state LWP (McCoy et al., 2022; Song et al., 2024; Tan et al., 2024).

In addition to the impact on the mean-state amount of cloud and resultant radiative properties, precipitation efficiency also plays an important role in setting the cloud macrophysical responses (ΔLWP) to warming and aerosol. Decreasing precipitation efficiency (increasing mean state LWP) corresponds to an increase in the LWP response to warming (Figure 2c: blue dots), which is broadly consistent with arguments related to moisture-convergence driven extratropical cloud feedback (McCoy et al., 2022; Tan et al., 2024). Similarly, decreasing precipitation efficiency (increasing mean state LWP) also corresponds to an increase in LWP response to changes in aerosol (Figure 2b: blue dots), consistent with simple arguments based on precipitation suppression from smaller and more abundant cloud droplets in the presence of more aerosols (Song et al., 2024). Comparing the cloud responses induced by aerosol and warming, a wider spread of LWP warming response relative to the LWP aerosol response is simulated across the CAM6 PPE (Figures 2a and 2b: blue dots). This is consistent with aerosol-cloud adjustments being dominated by precipitation suppression (Song et al., 2024) while cloud feedback is due to a combination of different processes such as changes in boundary layer structure (Terai et al., 2019), resulting in a wider variability in cloud response to warming. Taken together, the weaker variability in aerosol-driven liquid cloud response results in a fairly robust negative correlation between the LWP response to aerosol and the albedo susceptibility term (Figure S6b in Supporting Information S1) while the relationship is less robust between LWP response to warming and albedo susceptibility (Figure S6a in Supporting Information S1). Despite the difference in the strength of relationship, both the aerosol forcing (ERF_{aci}) and cloud radiative response to

warming ($\Delta CRE_{warming}$) can be predicted by the LWP responses scaled by albedo susceptibility (Figures 1a and 1b). However, the stronger negative relationship between LWP response to aerosols and albedo susceptibility relative to that from warming-driven changes, results in a stronger buffering of the magnitude of ERF_{aci} relative to $\Delta CRE_{warming}$ (Figure 1). This stronger buffering arises from a stronger decrease in albedo susceptibility to cloud responses due to aerosol (Figure S6 in Supporting Information S1).

Given the apparent role of precipitation efficiency in driving the correlation between ERF_{aci} and $\Delta CRE_{warming}$, we examine the precipitation efficiency as a function of parameters in Figure S7 in Supporting Information S1 to identify which parameters exert the strongest influence in models. We found the precipitation efficiency in the CAM6 PPE is primarily driven by variation in parameters related to precipitation process (Figure S7 in Supporting Information S1). The key parameterization of rain formation in CAM6 is through autoconversion. Autoconversion is used in representing initial rain formation in many ESMs in order to circumvent the need to deal with the complicated physical processes in micro-scale during rain formation (e.g., diabatic condensation and stochastic collection) (Gettelman et al., 2015; Khairoutdinov & Kogan, 2000; Lamb & Verlinde, 2011). The rate of generation of rain from cloud water through autoconversion in CAM6 is written as (Gettelman et al., 2015; Khairoutdinov & Kogan, 2000):

$$\left(\frac{\partial q_c}{\partial t}\right)_{\text{auto}} = a \cdot q_c^b \cdot Nd^{-c} \tag{10}$$

Where Nd is the cloud droplet concentration in cm^{-3}. q_c is the cloud water content in kg/kg. a, b and -c are uncertain parameters perturbed in the CAM6 PPE (Table S1 in Supporting Information S1). They are micro_mg_autocon_fact, micro_mg_autocon_lwp_exp and micro_mg_autocon_nd_exp, respectively. The positive correlation between micro_mg_autocon_nd_exp (i.e., -c in Equation 10) and precipitation efficiency with a *r*-value of 0.33 suggests that the precipitation is suppressed with decreasing (more negative) micro_mg_autocon_nd_exp (Figure S7-2 in Supporting Information S1). Precipitation efficiency also decreases with increasing micro_mg_autocon_lwp_exp with a r-value of −0.67 (Figure S7-21 in Supporting Information S1), as q_c is usually less than 1 kg/kg (Khairoutdinov & Kogan, 2000; Song et al., 2025). The results suggest that the buffering of cloud radiative response to aerosol (ERF_{aci}) and warming ($\Delta CRE_{warming}$) through precipitation efficiency are both primarily driven by the autoconversion parameterization in the CAM6. We note that the power law formulation of autoconversion is common across ESMs (Jing et al., 2019; Michibata & Takemura, 2015), suggesting the radiative buffering via precipitation efficiency may also occur in other models (McCoy et al., 2022; Song et al., 2024).

One caveat of CAM6 is that it does not include an explicit parameterized entrainment effect on clouds, which might suppress the compensation effect between LWP response and albedo susceptibility because the sedimentation–evaporation feedback tends to reduce LWP. Previous studies have shown entrainment can strongly affects both climate sensitivity (Rowlands et al., 2012) and aerosol forcing (Haerter et al., 2009). Nevertheless, we believe the radiative buffering effect identified in our study is not unique to CAM6, and likely persists in other models, including those with more explicit entrainment representations. More recent work shows that enhanced evaporation does not significantly reduce LWP (Karset et al., 2020), even when the emergent relationship between LWP and droplet number is negative (Mikkelsen et al., 2025; Mülmenstädt et al., 2024) and that positive LWP adjustments to aerosols are robust across models (Mülmenstädt et al., 2024).

3.3. Implications for Observational Constraints on Future Warming

The magnitude in future temperature change depends on the magnitude of the radiative forcings and feedbacks (Gregory et al., 2004). As discussed in Section 3.2, the precipitation processes determine precipitation efficiency (Figure S7 in Supporting Information S1), and result in macro-scale impacts on mean-state cloud amount (Figure S5 in Supporting Information S1). Precipitation efficiency also determines how that cloud interacts with top of atmosphere shortwave flux (Figures 2a and 2b: red dots), and the response of clouds to warming (Figure 2a: blue dots) and anthropogenic aerosol (Figure 2b: blue dots). We find a stronger compensation (or stronger negative correlation) between the cloud response and albedo susceptibility in aerosol-driven changes in cloud, relative to that from warming-driven changes (Figure S6 in Supporting Information S1), resulting in an emergent negative

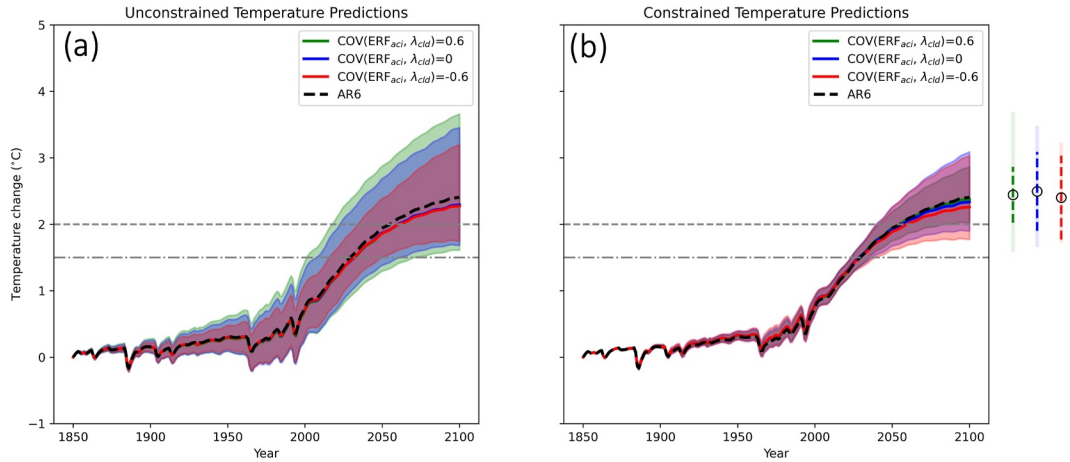

Figure 3. The surface mean temperature change under shared socioeconomic pathway 1–2.6 (SSP1-2.6) assuming three different correlations between ERF_{aci} and cloud feedback. (a) The 5–95th percentile range for each correlation scenario based on 1,000 ensembles. AR6 best estimates indicated in black dashed line. (b) Similar to (a) but showing ensembles that match with observed temperature records. The 5–95th percentile range of temperature change at the end of century is indicated to the right of the axis, with unconstrained ensembles from (a) shown in vertical solid lines and constrained ensembles from (b) shown in vertical dashed lines.

correlation between forcing from aerosol-cloud interactions ERF_{aci} and extratropical cloud feedback $\Delta CRE_{warming}$ (Figure 2d). What does this emergent correlation driven by shared processes mean for how we interpret ESMs?

Here we examine what an emergent relationship between ERF_{aci} and cloud feedback means for how we interpret a random prior distribution of ESMs. For the purposes of illustration, we provide a statistical exploration of how correlation between ERF_{aci} and cloud feedback affects our ability to predict future temperature trajectory and to provide observational constraints on future temperature trajectory.

Within the specific configuration for the FaIR model (Table S3 in Supporting Information S1), the means of the simulated temperature predictions with jointly sampled ERF_{aci} and cloud feedback (with r-value = −0.6, 0, 0.6) are consistent with the AR6 best estimates (Figure 3). This is not surprising as the FaIR model is tuned to match CESM2 (Watson-Parris, 2025) and the sampled aerosol forcing values are centered on the AR6 best estimate, leading the mean temperature projections to converge across correlation scenarios.

One emergent feature from our analysis is that a smaller uncertainty in future temperature change is simulated with FaIR model when ERF_{aci} and cloud feedback are anti-correlated. Assuming an imposed correlation of −0.6, the negative correlation reduces the likely range of temperature change in 2100 by 29%, comparing to the scenario of positive correlation (Figure 3a). The narrower range of the temperature change in anti-correlation scenario is expected as large positive ERF_{aci} is compensated with weaker cloud feedback to temperature change, and vice versa, leading to a relatively less spread in temperature projection. This is consistent with the negative correlation leading to compensation between the inter-model spreads of equilibrium climate sensitivities (C. Smith et al., 2021).

Another key insight is that the radiative forcing (through ERF_{aci}) have different impact on the prediction of future temperature change under different scenarios of correlations. When a negative correlation is imposed on ERF_{aci} and cloud feedback, a stronger (more negative) ERF_{aci} simulates a smaller warming before 2020 and a warmer future (after 2050) (Figure S8a in Supporting Information S1). The temperature prediction is consistent with the results in Watson-Parris and Smith (2022). However, the role of ERF_{aci} on future warming shifts when the correlation between ERF_{aci} and cloud feedback is positive or no correlation. When the imposed correlation is set to 0.6 or 0, strong ERF_{aci} shows a consistent cooling throughout the simulation years (Figures S8b and S8c in Supporting Information S1). This result highlights the importance of making assumptions on the dependence between forcing and feedback in inferring future warming.

Having explored the role of the range of historical ERF_{aci} in setting future warming in the context of temperature change, another question is how the correlation between our forcing and feedback priors impacts our

ability to constraining the uncertainty of future warming? Although the prior temperature change uncertainty is narrower in the case of negative correlation, we find that the uncertainty in the posterior temperature change shows more spread when ERF_{aci} and cloud feedback are anti-correlated (Figure 3b). Examination of the prior and posterior ERF_{aci} and cloud feedback distribution shows that ERF_{aci} and cloud feedback are the least constrained when the correlation is negative. There are 42% of ensembles in FaIR2.0 that simulate a temperature trajectory matched with historical temperature records when ERF_{aci} and cloud feedback are negatively correlated, while only 24% and 28% ensemble members agree with observations under conditions of positive correlation and no correlation. This indicates although a negative correlation produces a narrower range in future warming, negative correlations also make it easier to agree with historical record and harder to constrain future warming.

4. Conclusion

An emergent property from energy conservation is that forcing and feedback tend to be anticorrelated across fully-coupled climate models that have similar historical warming (Wang et al., 2021). However, we find a similar correlation in a perturbed parameter ensemble (PPE) where energy conservation is not enforced and members have no requirement to match a historical temperature trend. This correlation appears to be driven by cloud and precipitation processes (Gettelman et al., 2024) (Figures 1, 2a and 2b). We trace this negative correlation to precipitation efficiency in liquid cloud, which drives both aerosol-cloud adjustments through precipitation suppression (Song et al., 2024) (Figure 2a: blue dots) and cloud feedback driven by a strengthened hydrological cycle (McCoy et al., 2022; Werapitiya et al., 2025) (Figure 2b: blue dots). In addition to modulating liquid cloud responses to aerosol and warming, precipitation efficiency also modulates the radiative effect of changes in liquid clouds by setting the mean state LWP (Song et al., 2024) (Figures 2a and 2b: red dots).

We suggest that the compensation between LWP response (ΔLWP) and albedo susceptibility to LWP ($\partial\alpha/\partial LWP$) leads to a buffering in cloud radiative responses to both aerosol and warming (ERF_{aci} and $\Delta CRE_{warming}$). The stronger buffering on ERF_{aci} relative to $\Delta CRE_{warming}$ (Figure S6 in Supporting Information S1) leads to a negative correlation between ERF_{aci} and $\Delta CRE_{warming}$ (Figure 2d). One feature of the base model used in the PPE is that CAM6 exhibits a strong LWP response compared to other CMIP6 models (Gryspeerdt et al., 2020; Song et al., 2024). Similar behavior is also found in CAM5 (Gryspeerdt et al., 2020; Malavelle et al., 2017). This might raise the concern that our results are specific to the CAM model family. However, both CMIP5 and CMIP6 models exhibit a vast range of mean-state LWPs, consistent with the CAM6 PPE, and the radiative buffering is observed across these models (McCoy et al., 2022; Song et al., 2024). This suggests that radiative buffering effect is not an artifact of the PPE framework and is represented in ESMs. Another caveat of our study is that the analysis focuses on extratropical moisture-converging regions, where anthropogenic emissions are substantial and the moisture-convergence-driven cloud feedback is most relevant. While we do not expect the spatial pattern of aerosol emissions to be highly model dependent, the cloud feedback pattern, which is largely controlled by large-scale circulation, may still vary due to model-dependent processes and shifts in jet position, especially in free-running simulations.

Precipitation efficiency acting on both the cloud response to warming and aerosol as well as the mean-state cloud amount result in a negative correlation between forcing and feedback. Given that there is a physical mechanism driving this correlation, we need to characterize the implications for how we interpret climate models. We leverage a zero-dimensional energy balance model (FaIR2.0) to examine how correlations between ACI forcing (ERF_{aci}) and cloud feedback affect the uncertainty in future warming, and how the future projections under different scenarios of correlations (r-value $= -0.6$, 0 and 0.6) can be constrained by the historical temperature record. We find that by having a negative correlation between ERF_{aci} and cloud feedback, future warming shows less uncertainty (Figure 3a), and stronger ERF_{aci} (more negative) implies a hotter future (Figure S8a in Supporting Information S1). Instead, more uncertainty in future warming is predicted by FaIR2.0 when ERF_{aci} and cloud feedback are positively correlated or have no correlation, and stronger ERF_{aci} indicates a cooler future (Figures S8b and S8c in Supporting Information S1). We also find that although a negative correlation between priors of ERF_{aci} and cloud feedback shows less spread in historical temperature trajectory (Figure 3a), it also means that observations act as a weaker constraint on future warming (Figure 3b).

Given the above, reducing the uncertainty in future warming will likely require integrated analysis of satellite-derived radiation, cloud water content, precipitation, temperature and aerosol properties. However, it may not

be possible to fully disentangle their overlapping signals observationally. Determining precipitation efficiency from satellite observations or laboratory studies may offer an alternative constraint, and future work should explore whether such diagnostics can help narrow uncertainties in future warming.

Conflict of Interest

The authors declare no conflicts of interest relevant to this study.

Data Availability Statement

PPE data is available online (Eidhammer et al., 2024) and can be accessed through https://doi.org/10.26024/bzne-yf09. FaIRv2.0 was published by Leach et al. (2021), and the model code can be accessed through https://zenodo.org/records/4774994.

Acknowledgments
We would like to acknowledge the use of computational resources (https://doi.org/10.5065/D6RX99HX) at the NCAR-Wyoming Supercomputing Center provided by the National Science Foundation and the State of Wyoming, and supported by NCAR's Computational and Information Systems Laboratory. CS and DTM were supported by the U.S. Department of Energy's Regional and Global Modeling Analysis award DE-SC0025208. GW and DTM's efforts were supported under NASA Precipitation Measurement Mission Grant 80NSSC22K0609. The contributions of DTM were additionally supported by the U.S. Department of Energy's Atmospheric System Research Federal Award DE-SC002227 and U.S. Department of Energy's Established Program to Stimulate Competitive Research DE-SC0024161. DWP acknowledges funding from U.S. National Science Foundation award 2441832. The Pacific Northwest National Laboratory is operated for the U.S. Department of Energy by the Battelle Memorial Institute under contract DE-AC05-76RL01830.

References

Ackerman, A. S., Kirkpatrick, M. P., Stevens, D. E., & Toon, O. B. (2004). The impact of humidity above stratiform clouds on indirect aerosol climate forcing. *Nature*, *432*(7020), 1014–1017. https://doi.org/10.1038/nature03174

Albrecht, B. A. (1989). Aerosols, cloud microphysics, and fractional cloudiness. *Science*, *245*(4923), 1227–1230. https://doi.org/10.1126/science.245.4923.1227

Andrews, T., Gregory, J. M., Webb, M. J., & Taylor, K. E. (2012). Forcing, feedbacks and climate sensitivity in CMIP5 coupled atmosphere-ocean climate models. *Geophysical Research Letters*, *39*(9), L09712. https://doi.org/10.1029/2012gl051607

Bellouin, N., Quaas, J., Gryspeerdt, E., Kinne, S., Stier, P., Watson-Parris, D., et al. (2020). Bounding global aerosol radiative forcing of climate change. *Reviews of Geophysics*, *58*(1), e2019RG000660. https://doi.org/10.1029/2019rg000660

Boucher, O., Randall, D., Artaxo, P., Bretherton, C., Feingold, G., Forster, P., et al. (Eds.), Climate change 2013: The physical science basis. Contribution of working group i to the fifth assessment report of the intergovernmental panel on climate change (pp. 571–657). Cambridge, UK: Cambridge University Press. https://doi.org/10.1017/CBO9781107415324.016

Ceppi, P., Brient, F., Zelinka, M. D., & Hartmann, D. L. (2017). Cloud feedback mechanisms and their representation in global climate models. *Wiley Interdisciplinary Reviews: Climate Change*, *8*(4), e465. https://doi.org/10.1002/wcc.465

Cess, R. D., Potter, G. L., Blanchet, J., Boer, G., Ghan, S., Kiehl, J., et al. (1989). Interpretation of cloud-climate feedback as produced by 14 atmospheric general circulation models. *Science*, *245*(4917), 513–516. https://doi.org/10.1126/science.245.4917.513

Cummins, D. P., Stephenson, D. B., & Stott, P. A. (2020). Optimal estimation of stochastic energy balance model parameters. *Journal of Climate*, *33*(18), 7909–7926. https://doi.org/10.1175/jcli-d-19-0589.1

Danabasoglu, G., Lamarque, J.-F., Bacmeister, J., Bailey, D., DuVivier, A., Edwards, J., et al. (2020). The community Earth system model version 2 (cesm2). *Journal of Advances in Modeling Earth Systems*, *12*(2), e2019MS001916. https://doi.org/10.1029/2019ms001916

Eidhammer, T., Gettelman, A., Thayer-Calder, K., Watson-Parris, D., Elsaesser, G., Morrison, H., et al. (2024). An extensible perturbed parameter ensemble for the community atmosphere model version 6. *Geoscientific Model Development*, *17*(21), 7835–7853. https://doi.org/10.5194/gmd-17-7835-2024

Eyring, V., Bony, S., Meehl, G. A., Senior, C. A., Stevens, B., Stouffer, R. J., & Taylor, K. E. (2016). Overview of the coupled model intercomparison project phase 6 (cmip6) experimental design and organization. *Geoscientific Model Development*, *9*(5), 1937–1958. https://doi.org/10.5194/gmd-9-1937-2016

Forster, P. M. (2016). Inference of climate sensitivity from analysis of earth's energy budget. *Annual Review of Earth and Planetary Sciences*, *44*(1), 85–106. https://doi.org/10.1146/annurev-earth-060614-105156

Gettelman, A., Eidhammer, T., Duffy, M. L., McCoy, D. T., Song, C., & Watson-Parris, D. (2024). The interaction between climate forcing and feedbacks. *Journal of Geophysical Research: Atmospheres*, *129*(18), e2024JD040857. https://doi.org/10.1029/2024jd040857

Gettelman, A., Hannay, C., Bacmeister, J. T., Neale, R. B., Pendergrass, A., Danabasoglu, G., et al. (2019). High climate sensitivity in the community Earth system model version 2 (CESM2). *Geophysical Research Letters*, *46*(14), 8329–8337. https://doi.org/10.1029/2019gl083978

Gettelman, A., Morrison, H., Santos, S., Bogenschutz, P., & Caldwell, P. (2015). Advanced two-moment bulk microphysics for global models. Part ii: Global model solutions and aerosol–cloud interactions. *Journal of Climate*, *28*(3), 1288–1307. https://doi.org/10.1175/jcli-d-14-00103.1

Gregory, J. M., Ingram, W. J., Palmer, M., Jones, G. S., Stott, P., Thorpe, R., et al. (2004). A new method for diagnosing radiative forcing and climate sensitivity. *Geophysical Research Letters*, *31*(3), L03205. https://doi.org/10.1029/2003gl018747

Gryspeerdt, E., Mülmenstädt, J., Gettelman, A., Malavelle, F. F., Morrison, H., Neubauer, D., et al. (2020). Surprising similarities in model and observational aerosol radiative forcing estimates. *Atmospheric Chemistry and Physics*, *20*(1), 613–623. https://doi.org/10.5194/acp-20-613-2020

Haerter, J., Roeckner, E., Tomassini, L., & Von Storch, J.-S. (2009). Parametric uncertainty effects on aerosol radiative forcing. *Geophysical Research Letters*, *36*(15), L15707. https://doi.org/10.1029/2009gl039050

IPCC. (2023). *Summary for policymakers*. Geneva, Switzerland: IPCC. https://doi.org/10.59327/IPCC/AR6-9789291691647.001

Jing, X., Suzuki, K., & Michibata, T. (2019). The key role of warm rain parameterization in determining the aerosol indirect effect in a global climate model. *Journal of Climate*, *32*(14), 4409–4430. https://doi.org/10.1175/jcli-d-18-0789.1

Karset, I. H. H., Gettelman, A., Storelvmo, T., Alterskjær, K., & Berntsen, T. K. (2020). Exploring impacts of size-dependent evaporation and entrainment in a global model. *Journal of Geophysical Research: Atmospheres*, *125*(4), e2019JD031817. https://doi.org/10.1029/2019jd031817

Khairoutdinov, M., & Kogan, Y. (2000). A new cloud physics parameterization in a large-eddy simulation model of marine stratocumulus. *Monthly Weather Review*, *128*(1), 229–243. https://doi.org/10.1175/1520-0493(2000)128<0229:ancppi>2.0.co;2

Kiehl, J. T. (2007). Twentieth century climate model response and climate sensitivity. *Geophysical Research Letters*, *34*(22), L22710. https://doi.org/10.1029/2007gl031383

Lamb, D., & Verlinde, J. (2011). *Physics and chemistry of clouds*. Cambridge University Press.
Leach, N. J., Jenkins, S., Nicholls, Z., Smith, C. J., Lynch, J., Cain, M., et al. (2021). Fairv2. 0.0: A generalized impulse response model for climate uncertainty and future scenario exploration. *Geoscientific Model Development*, *14*(5), 3007–3036. https://doi.org/10.5194/gmd-14-3007-2021
Li, R. L., Studholme, J. H., Fedorov, A. V., & Storelvmo, T. (2022). Precipitation efficiency constraint on climate change. *Nature Climate Change*, *12*(7), 642–648. https://doi.org/10.1038/s41558-022-01400-x
Malavelle, F. F., Haywood, J. M., Jones, A., Gettelman, A., Clarisse, L., Bauduin, S., et al. (2017). Strong constraints on aerosol–cloud interactions from volcanic eruptions. *Nature*, *546*(7659), 485–491. https://doi.org/10.1038/nature22974
Mauritsen, T., Stevens, B., Roeckner, E., Crueger, T., Esch, M., Giorgetta, M., et al. (2012). Tuning the climate of a global model. *Journal of Advances in Modeling Earth Systems*, *4*(3), M00A01. https://doi.org/10.1029/2012ms000154
McCoy, D. T., Field, P., Frazer, M. E., Zelinka, M. D., Elsaesser, G. S., Mülmenstädt, J., et al. (2022). Extratropical shortwave cloud feedbacks in the context of the global circulation and hydrological cycle. *Geophysical Research Letters*, *49*(8), e2021GL097154. https://doi.org/10.1029/2021gl097154
Michibata, T., & Takemura, T. (2015). Evaluation of autoconversion schemes in a single model framework with satellite observations. *Journal of Geophysical Research: Atmospheres*, *120*(18), 9570–9590. https://doi.org/10.1002/2015jd023818-t
Mikkelsen, A., McCoy, D. T., Eidhammer, T., Gettelman, A., Song, C., Gordon, H., & McCoy, I. L. (2025). Constraining aerosol–cloud adjustments by uniting surface observations with a perturbed parameter ensemble. *Atmospheric Chemistry and Physics*, *25*(8), 4547–4570. https://doi.org/10.5194/acp-25-4547-2025
Molod, A., Takacs, L., Suarez, M., & Bacmeister, J. (2015). Development of the geos-5 atmospheric general circulation model: Evolution from merra to merra2. *Geoscientific Model Development*, *8*(5), 1339–1356. https://doi.org/10.5194/gmd-8-1339-2015
Mülmenstädt, J., Gryspeerdt, E., Dipu, S., Quaas, J., Ackerman, A. S., Fridlind, A. M., et al. (2024). General circulation models simulate negative liquid water path–droplet number correlations, but anthropogenic aerosols still increase simulated liquid water path. *Atmospheric Chemistry and Physics*, *24*(12), 7331–7345. https://doi.org/10.5194/acp-24-7331-2024
Qin, Y., Zelinka, M. D., & Klein, S. A. (2022). On the correspondence between atmosphere-only and coupled simulations for radiative feedbacks and forcing from co2. *Journal of Geophysical Research: Atmospheres*, *127*(3), e2021JD035460. https://doi.org/10.1029/2021jd035460
Ringer, M., Martin, G., Greeves, C., Hinton, T., James, P., Pope, V., et al. (2006). The physical properties of the atmosphere in the new hadley centre global environmental model (hadgem1). Part ii: Aspects of variability and regional climate. *Journal of Climate*, *19*(7), 1302–1326. https://doi.org/10.1175/jcli3713.1
Rowlands, D. J., Frame, D. J., Ackerley, D., Aina, T., Booth, B. B., Christensen, C., et al. (2012). Broad range of 2050 warming from an observationally constrained large climate model ensemble. *Nature Geoscience*, *5*(4), 256–260. https://doi.org/10.1038/ngeo1430
Senior, C., & Mitchell, J. (1993). Carbon dioxide and climate. The impact of cloud parameterization. *Journal of Climate*, *6*(3), 393–418. https://doi.org/10.1175/1520-0442(1993)006<0393:cdacti>2.0.co;2
Sexton, D. M., McSweeney, C. F., Rostron, J. W., Yamazaki, K., Booth, B. B., Murphy, J. M., et al. (2021). A perturbed parameter ensemble of hadgem3-gc3. 05 coupled model projections: Part 1: Selecting the parameter combinations. *Climate Dynamics*, *56*(11), 3395–3436. https://doi.org/10.1007/s00382-021-05709-9
Sherwood, S. C., Webb, M. J., Annan, J. D., Armour, K. C., Forster, P. M., Hargreaves, J. C., et al. (2020). An assessment of earth's climate sensitivity using multiple lines of evidence. *Reviews of Geophysics*, *58*(4), e2019RG000678. https://doi.org/10.1029/2019rg000678
Smith, C., Forster, P., Palmer, M., Collins, B., Leach, N., & Watanabe, M. (2021). *Ipcc-wg1/chapter-7: Ipcc wgi ar6 chapter 7 (v. 1.0)*. Zenodo.
Smith, C. J., Kramer, R. J., Myhre, G., Alterskjær, K., Collins, W., Sima, A., et al. (2020). Effective radiative forcing and adjustments in cmip6 models. *Atmospheric Chemistry and Physics*, *20*(16), 9591–9618. https://doi.org/10.5194/acp-20-9591-2020
Soden, B., & Chung, E.-S. (2017). The large-scale dynamical response of clouds to aerosol forcing. *Journal of Climate*, *30*(21), 8783–8794. https://doi.org/10.1175/jcli-d-17-0050.1
Soden, B. J., Broccoli, A. J., & Hemler, R. S. (2004). On the use of cloud forcing to estimate cloud feedback. *Journal of Climate*, *17*(19), 3661–3665. https://doi.org/10.1175/1520-0442(2004)017<3661:otuocf>2.0.co;2
Soden, B. J., & Held, I. M. (2006). An assessment of climate feedbacks in coupled ocean–atmosphere models. *Journal of Climate*, *19*(14), 3354–3360. https://doi.org/10.1175/jcli3799.1
Song, C., McCoy, D. T., Eidhammer, T., Gettelman, A., McCoy, I. L., Watson-Parris, D., et al. (2024). Buffering of aerosol-cloud adjustments by coupling between radiative susceptibility and precipitation efficiency. *Geophysical Research Letters*, *51*(11), e2024GL108663. https://doi.org/10.1029/2024gl108663
Song, C., McCoy, D. T., McCoy, I. L., Brown, H., Gettelman, A., Eidhammer, T., & Barahona, D. (2025). Aircraft in-situ measurements from socrates constrain the anthropogenic perturbations of cloud droplet number. *EGUsphere*, *2025*(22), 1–30. https://doi.org/10.5194/acp-25-16063-2025
Stephens, G. L. (1978). Radiation profiles in extended water clouds. ii: Parameterization schemes. *Journal of the Atmospheric Sciences*, *35*(11), 2123–2132. https://doi.org/10.1175/1520-0469(1978)035⟨2123:RPIEWC⟩2.0.CO;2
Tan, C., McCoy, D. T., & Elsaesser, G. S. (2024). Constraints on southern ocean shortwave cloud feedback from the hydrological cycle. *Journal of Geophysical Research: Atmospheres*, *129*(6), e2023JD040489. https://doi.org/10.1029/2023jd040489
Taylor, K. E., Stouffer, R. J., & Meehl, G. A. (2012). An overview of CMIP5 and the experiment design. *Bulletin of the American Meteorological Society*, *93*(4), 485–498. https://doi.org/10.1175/bams-d-11-00094.1
Terai, C., Zhang, Y., Klein, S., Zelinka, M., Chiu, J., & Min, Q. (2019). Mechanisms behind the extratropical stratiform low-cloud optical depth response to temperature in arm site observations. *Journal of Geophysical Research: Atmospheres*, *124*(4), 2127–2147. https://doi.org/10.1029/2018jd029359
Twomey, S. (1977). The influence of pollution on the shortwave albedo of clouds. *Journal of the Atmospheric Sciences*, *34*(7), 1149–1152. https://doi.org/10.1175/1520-0469(1977)034<1149:tiopot>2.0.co;2
Wall, C. J., Norris, J. R., Possner, A., McCoy, D. T., McCoy, I. L., & Lutsko, N. J. (2022). Assessing effective radiative forcing from aerosol–cloud interactions over the global ocean. *Proceedings of the National Academy of Sciences*, *119*(46), e2210481119. https://doi.org/10.1073/pnas.2210481119
Wang, C., Soden, B. J., Yang, W., & Vecchi, G. A. (2021). Compensation between cloud feedback and aerosol-cloud interaction in cmip6 models. *Geophysical Research Letters*, *48*(4), e2020GL091024. https://doi.org/10.1029/2020gl091024
Watson-Parris, D. (2025). Integrating top-down energetic constraints with bottom-up process-based constraints for more accurate projections of future warming. *Geophysical Research Letters*, *52*(8), e2024GL114269. https://doi.org/10.1029/2024gl114269
Watson-Parris, D., & Smith, C. J. (2022). Large uncertainty in future warming due to aerosol forcing. *Nature Climate Change*, *12*(12), 1111–1113. https://doi.org/10.1038/s41558-022-01516-0

Webb, M. J., Lambert, F. H., & Gregory, J. M. (2013). Origins of differences in climate sensitivity, forcing and feedback in climate models. *Climate Dynamics*, *40*(3–4), 677–707. https://doi.org/10.1007/s00382-012-1336-x

Werapitiya, G., McCoy, D. T., Elsaesser, G. S., Gettelman, A., Eidhammer, T., Aerenson, T., et al. (2025). Extratropical cloud feedback constrained by cloud sources and sinks in cyclones. *Journal of Climate*, *38*(24), 7285–7300. https://doi.org/10.1175/JCLI-D-24-0607.1

Zelinka, M. D., Myers, T. A., McCoy, D. T., Po-Chedley, S., Caldwell, P. M., Ceppi, P., et al. (2020). Causes of higher climate sensitivity in cmip6 models. *Geophysical Research Letters*, *47*(1), e2019GL085782. https://doi.org/10.1029/2019gl085782